

https://dspace.org/

The shape of sand particles Assessments of threedimensional form and angularity

Alvino Bezuidenhout; Muhammad Bodhania; Lerato Tiroyabone; Cara Eddey; Luis Alberto Torres Cruz

https://hdl.handle.net/10539/40585
WOS

Downloaded from a DSpace repository. https://dspace.org/

HOSTED BY
ELSEVIER
Available online at www.sciencedirect.com
ScienceDirect
Soils and Foundations 64 (2024) 101437
www.elsevier.com/locate/sandf

Technical Paper

The shape of sand particles: Assessments of three-dimensional form and angularity

A.W. Bezuidenhout, M. Bodhania, L. Tiroyabone, C. Eddey, L.A. Torres-Cruz *

School of Civil and Environmental Engineering, University of the Witwatersrand, Johannesburg, South Africa

Received 2 March 2023; received in revised form 15 January 2024; accepted 1 February 2024

Abstract

Particle shape affects the mechanical behaviour of soil and is thus a parameter of interest in geotechnical engineering. Shape is commonly described by form, angularity and roughness. Form describes the overall aspect ratio, angularity the sharpness of the edges and corners, and roughness the small surface irregularities. This work explores the characterisation of form and angularity of sand particles. Our results show that focus variation microscopy principles can be implemented in a conventional compound microscope to measure particle heights as small as 60 μm without having to observe a lateral view of the particle. The robustness of the procedure is demonstrated by implementing it on sand-sized particles from six different sources. Importantly, the compound microscope employed by the procedure is likely to be accessible to many soil laboratories. Heights measured using focus variation were used to assess particle form. Contrary to assumptions in previous works, form varied significantly within a given soiltype and a narrow particle size range. Regarding angularity, there is a systematic correlation between particle form and the angularity metric known as 'ellipseness'. Furthermore, while ellipseness is adequate to distinguish between angular and rounded particles, it cannot distinguish between sub-rounded and well-rounded particles.
© 2024 Production and hosting by Elsevier B.V. on behalf of The Japanese Geotechnical Society. This is an open access article under the CC BY license (http://creativecommons.org/licenses/by/4.0/).

Keywords: Particle shape; Three-dimensional form; Angularity; Ellipseness; Roundness; Focus variation

1. Introduction

Particle shape has a significant influence on the mechanical properties of soil and is thus an aspect of interest to geotechnical engineers (Holtz and Kovacs, 1981; Cho et al., 2006; Clayton et al., 2009; Shin and Santamarina, 2013). It is common to describe particle shape in terms of three independent aspects: form, angularity, and roughness. Form describes the overall aspect ratio, angularity characterises the sharpness of corners and edges, and roughness refers to the surface texture (Barret, 1980; Cho et al., 2006; Clayton et al., 2009). The current work extends the validity of a novel method that enables the three-dimensional (3D) characterisation of the form of sand-sized particles and explores the use of an existing 'ellipseness' parameter to quantify angularity.

Descriptors of form should ideally consider the 3D nature of particles. This requires the measurement of their shortest (S), intermediate (I) and longest (L) dimensions (Blott and Pye, 2008). S, I and L can then be used to compute multiple form parameters (e.g. Wentworth, 1922; Zingg, 1935; Krumbein, 1941; Corey, 1949; Aschenbrenner, 1956; Sneed and Folk, 1958; Dobkins and Folk, 1970; Clayton et al., 2009) and to plot the particle in a form characterisation diagram (e.g. Zingg, 1935; Sneed and Folk, 1958). This 3D characterisation of particle form is relevant to geotechnical engineers because 3D form affects mechanical behaviour. For instance, bulky particles

* Corresponding author.
E-mail address: LuisAlberto.TorresCruz@wits.ac.za (L.A. Torres-Cruz).

https://doi.org/10.1016/j.sandf.2024.101437
0038-0806/© 2024 Production and hosting by Elsevier B.V. on behalf of The Japanese Geotechnical Society.
This is an open access article under the CC BY license (http://creativecommons.org/licenses/by/4.0/).

behave differently from platy particles (Clayton et al., 2009).

In the case of sand-sized particles, their small dimensions require the use of a microscope to perform particle size measurements. There are several approaches available to estimate two of the dimensions S, I and L from the plan view of a sand-sized particle as observed under a microscope (Blott and Pye, 2008). However, the 'height' of the particle, which is parallel to the line of view, is hidden from the observer and thus cannot be directly measured on a static image of the plan view. Direct measurement of the height thus requires rotating the particle to reveal a lateral view (Clayton et al., 2009; Le Pen et al., 2013; Eddey et al., 2019). While conceptually simple, this is a relatively time-consuming process that is not often performed. In fact, the practical difficulty of capturing the 3D form of particles has led to the development of multiple two-dimensional (2D) form descriptors (Wadell, 1933; Riley, 1941; Pye and Pye, 1943; Cho et al., 2006; Clayton et al., 2009).

Notwithstanding the success of correlating 2D form descriptors to mechanical behaviour (Cho et al., 2006), efforts to develop methods capable of accounting for the 3D shape of particles have continued. For instance, laser scanning can successfully reproduce the particle morphology of gravel-sized particles (Lee et al., 2007; Mgangira et al., 2013; Sun et al., 2014; Nie et al., 2018; Cruz-Matías et al., 2019). However, limitations in resolution render the technique inapplicable to sand-sized particles. Micro computed tomography (μCT) is a powerful technique that can successfully characterise the shape of sand-sized particles (Fonseca et al., 2012; Alshibli et al., 2014; Zhao et al., 2015; Zhou and Wang, 2016; Yu et al., 2018; Zhou et al., 2018; Liang et al., 2021). Unfortunately, the specialised equipment required by this technique places it out of the reach of many researchers and practitioners.

Other methods that account for the 3D form of particles estimate the height based on a plan view, the mass, and an assumption regarding the shape of the particles (e.g. Kwan et al., 1999; Clayton et al., 2009). These methods have the advantage of being able to inspect multiple particles at once, however, their disadvantage is that they produce a single average indicator of form that does not reflect the potential variability within the sample.

An alternative approach is the application of focus variation principles which has proven useful to perform 3D form characterisations of gravel-sized particles (Masad, 2005). Additionally, preliminary results suggest that focus variation microscopy has the potential to aid in the 3D form characterisation of sand-sized particles (Eddey et al., 2019). Focus variation microscopy exploits the limited depth of field (DoF) of an optical system to measure distances that are parallel to the line of view. The DoF is "*the axial depth of the space on both sides of the object plane within which the object can be moved without detectable loss of sharpness in the image...*" (ISO, 2020). This is essentially the distance between the closest and farthest planes perpendicular to the line of view that are in sharp focus.

The very small DoF of specialised focus variation microscopes makes them capable of detecting surface irregularities in the range of micro- and nanometres (e.g. Scherer, 2007; Danzl et al., 2009; Jumelle et al., 2017). Measurements on platinum tailings indicate that although conventional compound microscopes have a larger DoF than specialised focus variation instruments, their DoF is still small enough that it is possible to use principles of focus variation microscopy to measure particle heights greater than 520 μm without directly observing a lateral view (Eddey et al., 2019). This is a promising approach because conventional compound microscopes are much more affordable, and thus accessible, than μCT scanners or specialised focus variation microscopes. However, the focus variation approach has not been validated for particle heights smaller than 520 μm.

The second aspect of particle shape considered herein is angularity, or its inverse roundness. The roundness index (R) proposed by Wadell (1932) is based on the 2D projection of a particle and is often the basis of visual comparators developed to expedite angularity assessments (Krumbein, 1941; Powers, 1953; Krumbein and Sloss, 1963; Cho et al., 2006; Blott and Pye, 2008; ASTM, 2017). Roundness is defined as

$$R = \frac{\sum D_i/n}{D_{ic}} \tag{1}$$

where D_i takes on the value of the diameter of curvature of all the corners identified on the outline of the particle, n is the total number of corners, and D_{ic} is the diameter of the maximum inscribed circle within the outline of the particle (Fig. 1). In this definition of roundness R, a 'corner' is any

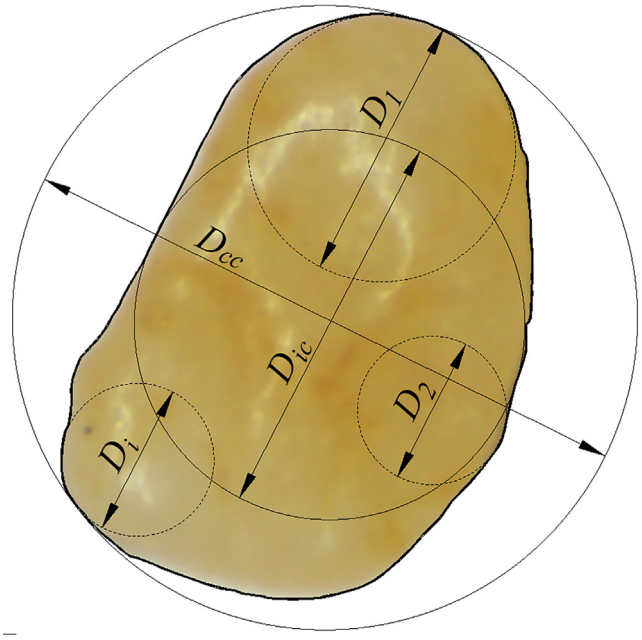


Fig. 1. Particle of East London Beach sand showing the diameters of the maximum inscribed and minimum circumscribed circles (D_{ic} and D_{cc}, respectively), and the curvature of the corners (D_i).

such feature whose diameter of curvature does not exceed D_{ic} (Wadell, 1932). Roundness R, as defined by Eq. (1), is independent of particle form. This was emphasised by Blott and Pye (2008) who noted that while a perfect circle yields $R = 1$, so does a rectangle whose ends consist of semicircles. Conversely, a regular dodecagon, whose overall form closely resembles a circle, yields $R = 0$ because its corners have a diameter of curvature $D_i = 0$.

Previous researchers have noted that the calculation of Wadell's roundness is time-consuming and can be hindered by subjective judgements of the location and curvature of corners (Janoo, 1998; Blott and Pye, 2008; Le Pen et al., 2013). To overcome these objections, the ellipseness (E) parameter was proposed as a simpler alternative to Wadell's roundness (Le Pen et al., 2013). Like Wadell's roundness, ellipseness is also based on a 2D projection of the particle and is defined as

$$E = \frac{P_e}{P_0} \tag{2}$$

where P_0 is the perimeter of the particle, and P_e is the perimeter of an ellipse with an area (A) equal to the area of the 2D projection of the particle, and a major radius (a) equal to half of the length of the longest line joining two points on the particle perimeter and passing through its centroid. Le Pen et al. (2013) noted that E approaches a maximum value of 1 as the particle outline becomes more ellipse-like. Conversely, E can in principle approach zero in particles with a very jagged outline that leads to $P_e << P_0$. As there is no closed-form formula for the perimeter of an ellipse P_e, Le Pen et al. (2013) worked with the approximation presented in Eq. (3) originally proposed by Ramanujan (1914).

$$P_e \approx \pi(a+b)\left(1 + \frac{3\left(\frac{a-b}{a+b}\right)^2}{10 + \sqrt{4 - 3\left(\frac{a-b}{a+b}\right)^2}}\right) \tag{3}$$

where $b = A/\pi a$ is the minor radius of the ellipse.

The current paper contributes to the characterisation of the form and angularity of sand-sized particles as follows. We explore the ability of the focus variation microscopy approach, previously used to measure particle heights as small as 520 μm (Eddey et al., 2019), to measure smaller particle heights. We substantiate the robustness of the procedure by implementing it on particles from six different sources in addition to iron filings which aided the validation of the method. We also use the focus variation approach to perform 3D characterisations of particle form and gain insights into its variability and correlation with particle size. Regarding angularity, the paper explores the correlation between ellipseness E and particle form as well as the suitability of ellipseness E to characterise the angularity of a variety of sand types.

2. Materials and methods

2.1. Particle types

Seven particle types covering a variety of sources were considered herein and are listed in Table 1. The East London Beach sand and Ballito Beach sand are sea sands that originate from the South African provinces of Eastern Cape and KwaZulu-Natal, respectively. The crushed quartz sand is a commercial product typically used as a swimming pool filter. The platinum tailings were collected from a mine in the South African province of North West. The Vaal River sand was collected ~15 km upstream from the town of Parys, South Africa. The glass beads are commercially available for use as an additive in reflective paints. The iron filings were sourced from a metal workshop. Fig. 2 presents micrographs of all the particle types except the iron filings which, as described below, were used exclusively to aid the validation of the focus variation procedure. All particles passed the 2.36 mm sieve and were retained in the 75 μm sieve. Additional intermediate sieves facilitated the selection of particle sizes that were approximately uniformly distributed within this size range.

2.2. Experimental setup

A Nikon Optiphot-Pol optical compound microscope (Fig. 3) like the one used in Eddey et al. (2019) was used to examine all particles. A universal epi-illuminator accessory provided a bright and uniformly illuminated view of the particles. The microscope field of view was digitised with a 2592 × 1944-pixel complementary metal–oxide–semiconductor (CMOS) sensor which had square pixels with side $e = 2.2$ μm. The NIS-Elements 4.0 version D software was used to capture the micrographs and perform measurements. Table 2 summarises the magnification, numerical aperture and depth of field DoF of the four objectives fitted to the microscope. The magnification of each objective was enhanced by the 10x magnification of the ocular lens to yield total magnifications of 50x, 100x, 200x and 400x. The depth of field DoF is a key feature because the successful implementation of a focus variation approach to measure particle height requires a limited DoF. Several equations exist in the literature to compute the DoF (Goodwin, 2015). Herein we use Eq. (4) proposed by Inoué and Spring (1997).

$$DoF = \frac{\lambda \cdot n}{NA^2} + \frac{n}{M \cdot NA} e \tag{4}$$

where λ is the wavelength of the illuminating light, n is the lowest refractive index of the media between the objective and the sand particle, NA is the numerical aperture of the objective, M is the magnification of the objective, and e is pixel spacing. Herein, DoF calculations adopted $n = 1$ (air) and a characteristic value of $\lambda = 0.55$ μm.

Prior to their inspection under the microscope, particles were placed one at a time on a prismatic base. The larger

Table 1
Number of particles used for different aspects of the experimental programme.

Material type	Number of particles used for:			
	Validation of focus variation procedure	Form assessment	Assessments of roundness and ellipseness	Total[a]
East London Beach sand	50	50	15	65
Ballito Beach sand	50	50	15	65
Crushed quartz sand	70	150	10	180
Platinum tailings	57	162	10	179
Vaal River sand	20	70	0	90
Glass beads	20	20	10	30
Iron filings	19	0	0	19
Total	286	502	60	628

Note: a) Because some particles were used for more than one purpose, the total number of particles per material type is not equal to the addition of the row.

particles were moved by hand, but smaller particles required the use of tweezers and a hand lens.

Once ready for inspection under the microscope, particles were analysed for at least one of the following purposes: 1) validation of the focus variation procedure, 2) assessment of form, 3) assessment of roundness R and ellipseness E. Table 1 indicates the number of particles analysed for each purpose. The description of these procedures follows.

2.3. Validation of the focus variation procedure

The objective of the focus variation procedure is to determine the height of the particle as it sits on the prismatic base without having to observe a lateral view. The particle height is the vertical distance between the surface on which the particle sits and the uppermost tip of the particle. For this purpose, the coarse and fine focus knobs of the microscope were used to move the stage vertically to an initial position in which only the uppermost part of a particle was in focus. That is, a position in which any further lowering of the stage resulted in the whole particle going out of focus (Fig. 4a). Subsequently, the fine focus knob was operated to move the stage upwards causing increasingly lower portions of the particle to come into focus (Fig. 4b to Fig. 4c) until the particle itself was out of focus but the horizontal surface on which it rested was in sharp focus (Fig. 4d). The natural texture of the surface underlying the particle facilitated the determination of the stage position at which such surface came into sharp focus (Fig. 4d). The vertical displacement of the stage that shifted the focus from the upper tip of the particle to the surface of the prismatic base was termed $D_{\Delta f}$ and was equated to the height of the particle. All focus adjustments were based on visual inspection of the images which introduces some uncertainty due to subjectivity.

The vertical displacement of the stage was measured using one of two approaches. Initially, the measurement relied on the microscope's built-in fine focus knob which had divisions corresponding to displacements of 1 μm. However, to eliminate reliance on the specific characteristics of the microscope, this measurement approach was replaced by a standalone dial indicator with a 1 μm resolution (Fig. 3). The verticality of the dial indicator was ensured with the aid of a spirit level.

To validate the particle height inferred from the focus variation procedure ($D_{\Delta f}$), the prismatic base was turned on its side to measure particle height directly from two mutually orthogonal lateral views. Particles were placed close to a corner of the prismatic base to facilitate unobstructed lateral views. In principle, the heights inferred from the two lateral views should be equal but in practice some discrepancies are unavoidable. Accordingly, the smaller and larger of these measurements were termed D_{L1} and D_{L2}, respectively, and their mean value was termed D_L.

Inspection of lateral views required fixing the particle to the prismatic base to prevent the particle from falling upon rotation of the base. This was done in one of two ways. For the iron filings, one face of the prismatic base was covered with a magnetic adhesive tape. The magnetic attraction between the iron filings and the tape effectively fixed the particle. For all other particle types, a thin layer of solid or liquid adhesive spread thinly with the finger on the prismatic base created the bond between particle and base. By using both approaches it was possible to investigate whether the thickness of the adhesive layer was detrimental to the accuracy of the particle height measurements using the focus variation procedure. Some of the smallest particles were positioned on the base by first placing the particle on a sheet of clean paper, then applying the glue on the base and finally gently pressing the glue-covered face of the base against the particle.

2.4. Assessments of form

Assessments of form required the determination of the particle dimensions S, I and L. There are multiple ways to determine these dimensions (Blott and Pye, 2008) and the approach adopted herein assumes that the particle height as measured by the focus variation procedure ($D_{\Delta f}$) is one of the three required dimensions. Following previous works (Clayton et al., 2009; Le Pen et al., 2013; Eddey et al., 2019; Wang et al., 2020), the two remaining

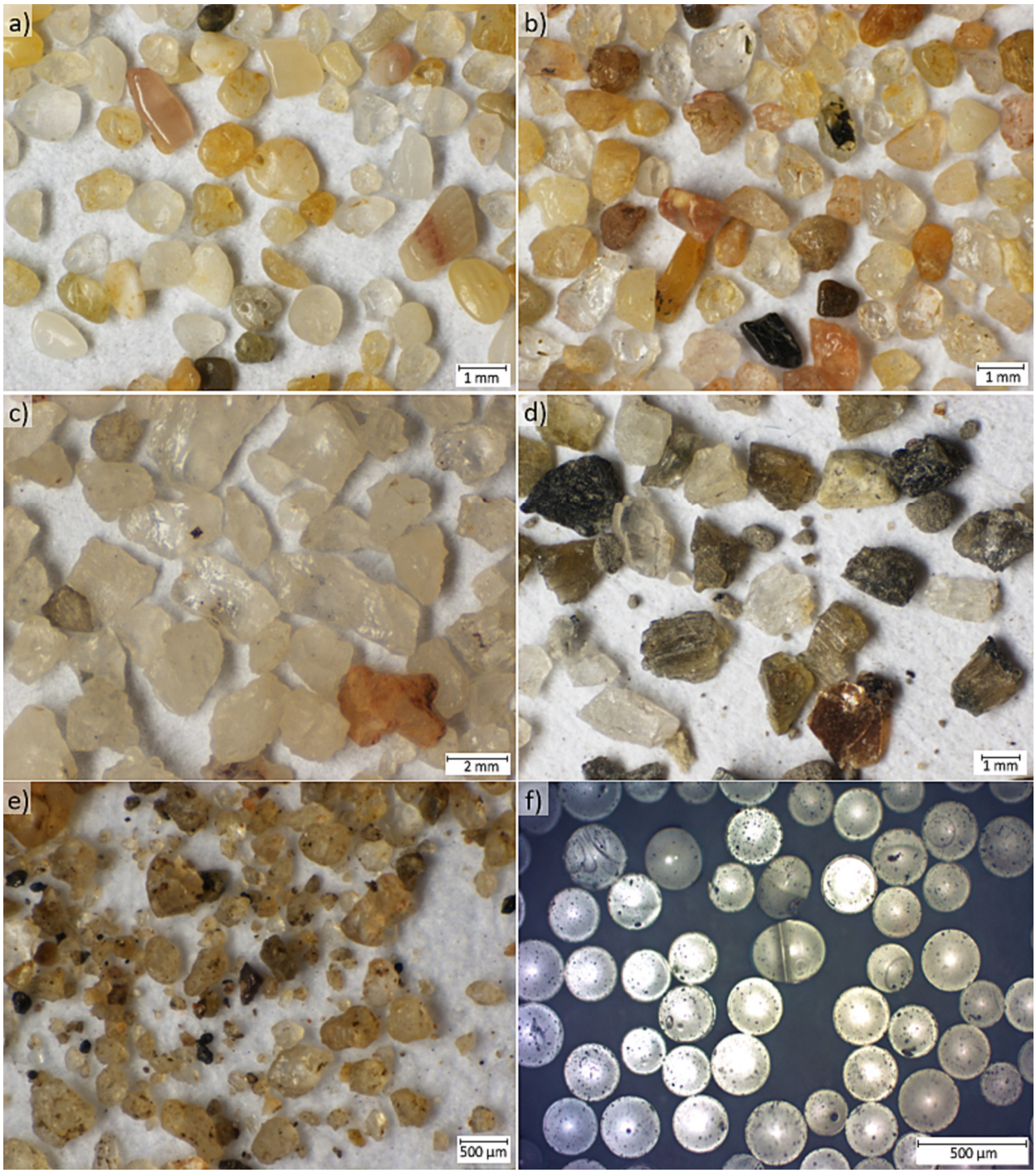


Fig. 2. Micrographs of: (a) East London Beach sand; (b) Ballito Beach sand; (c) crushed quartz sand; (d) platinum tailings; (e) Vaal River sand; and (f) glass beads.

dimensions were taken to be equal to the diameters of the maximum inscribed (D_{ic}) and minimum circumscribed (D_{cc}) circles in the plan view of the particle (Fig. 1). $D_{\Delta f}$, D_{ic}, and D_{cc} were then assigned to S, I and L ensuring that $S \leq I \leq L$. Because particles tended to lie on their most mechanically stable position when placed on the prismatic base, it was generally the case that $D_{\Delta f} = S$, $D_{ic} = I$, *and* $D_{cc} = L$.

2.5. Assessments of roundness and ellipseness

The investigation into a potential effect of form on ellipseness E relied on a particle outline idealised as shown in Fig. 5. The idealised outline is essentially a rectangle with four rounded corners exhibiting the same diameter of curvature (D) which can vary from 0 to D_{ic}. The round-

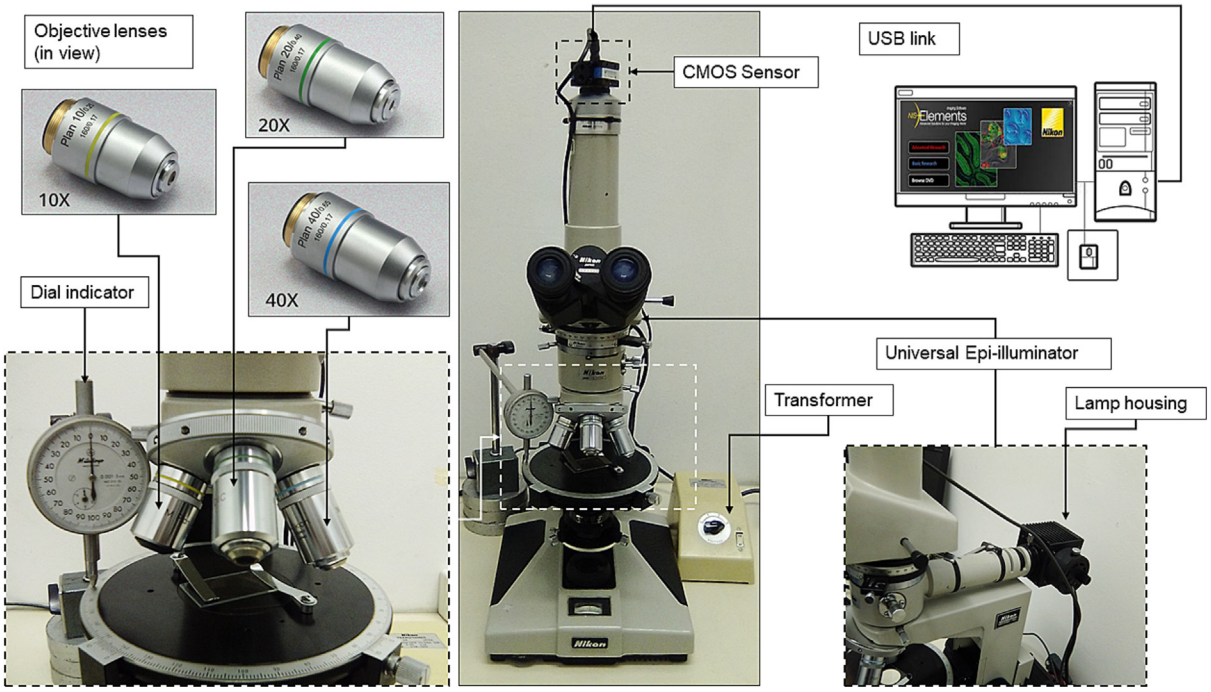


Fig. 3. Experimental setup.

Table 2
Characteristics of each objective lens.

Objective Magnification	Objective Numerical Aperture	Depth of Field (μm)
5	0.10	59
10	0.25	9.7
20	0.40	3.7
40	0.65	1.4

ness R, major radius a and perimeter P_0 of the idealised outline are given by

$$R = \frac{D}{D_{ic}} \tag{5}$$

$$a = \frac{\sqrt{(w-D)^2 + (h-D)^2} + D}{2} \tag{6}$$

$$P_0 = 2(w-D) + 2(h-D) + \pi D \tag{7}$$

where w and h are the width and height of the rectangle, respectively (Fig. 5).

Adopting the ratio h/w to characterise the overall form of the idealised particle outline, the effect of form on E can be investigated by deriving an expression for E as a function of h/w. However, the authors found this analytical approach intractable and opted instead for a numerical approach in which, for a given roundness R, the ellipseness E of the idealised outline was computed for 121 discrete values of (w, h). These discrete values resulted from considering all possible (w, h) combinations that emerge when w and h can take on 0.1 and on all integer values from 1 to 10. This yielded a maximum and minimum h/w ratio of $10/0.1 = 100$ and $0.1/10 = 0.01$. For each (w, h) combination, roundness values of $R = 0$, 0.5, and 1 were considered. The results, discussed below, enabled the investigation of the relationship between E and the form ratio h/w.

Moving from idealised outlines to real particles, the angularity metrics R and E were computed by implementing Eqs. (1) and (2), respectively, on the plan view outline of 60 particles selected from five material types as shown in Table 1. All particles passed the 1180 μm sieve and were retained in the 600 μm sieve. The fractal nature of particle outlines implies that the measured perimeter P_0 depends on the level of magnification, with higher magnifications yielding ever-increasing estimates of P_0 (Orford and Whalley, 1983). To mitigate the possible variability that can be introduced by this effect, all R and E measurements were conducted at the same total magnification of 50x.

3. Results and discussion

3.1. Validation of the focus variation procedure

Fig. 6 compares the particle heights inferred from the focus variation procedure $D_{\Delta f}$ to the mean of the particle

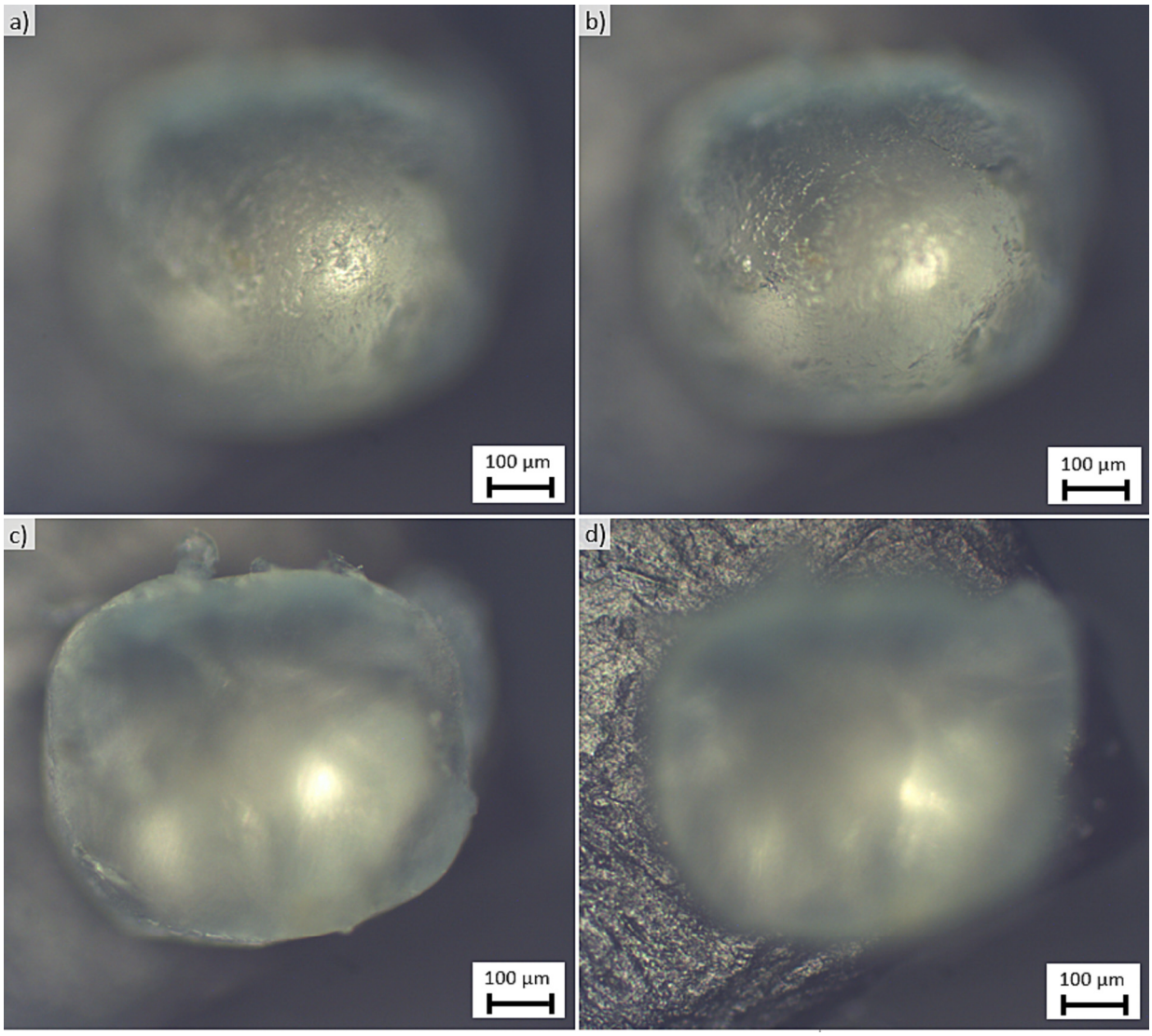


Fig. 4. The focus variation procedure from (a) the start of the procedure with the uppermost part of the particle in focus; to (d) the end of the procedure with the base in focus.

heights measured from two lateral views D_L. Excellent agreement is observed between the two approaches for all material types. The results include only two particles with $D_{\Delta f} < 100$ µm which reflects the difficulty of handling small particles. However, the smallest $D_{\Delta f}$ is of ~60 µm which we suggest is the lower bound of applicability of the procedure. This lower bound is similar to the sand-silt boundary typically adopted in soil classification systems. Considering that the largest $D_{\Delta f}$ is of 1175 µm, the results support the validity of the method for particle heights 60 µm $\leq D_{\Delta f} \leq$ 1200 µm. This range represents a significant reduction of the lower bound of application validated in previous investigations which was 520 µm $\leq D_{\Delta f} \leq$ 1200 µm (Eddey et al., 2019). While our results do not modify the validated upper bound of the procedure (1200 µm), we do not anticipate difficulties in larger particles if they remain small enough to be inspected with a compound microscope.

A previously proposed method to assess particle form relied on estimates of the volume equivalent minor dimension of a scalene ellipsoid (S_{vse}) (Clayton et al., 2009). As this suggests, the method idealises particle geometry as a scalene ellipsoid, i.e. an ellipsoid whose three principal axes have different sizes. Although, the scalene ellipsoid method provides a single average value of S/L for a sample of multiple particles, its validation involved measurements on 36 individual particles for which S_{vse} was compared to the D_{ic} measured on a lateral view (Clayton et al., 2009). Fig. 6 includes this dataset and shows that its scatter around the 1:1 line is significantly larger than that of the measurements performed using the focus variation procedure. It follows that focus variation can better estimate the height of the particle than the scalene ellipsoid procedure can estimate the D_{ic} of a side view.

While Fig. 6 enables an initial assessment of the precision of $D_{\Delta f}$, a more rigorous assessment requires acknowl-

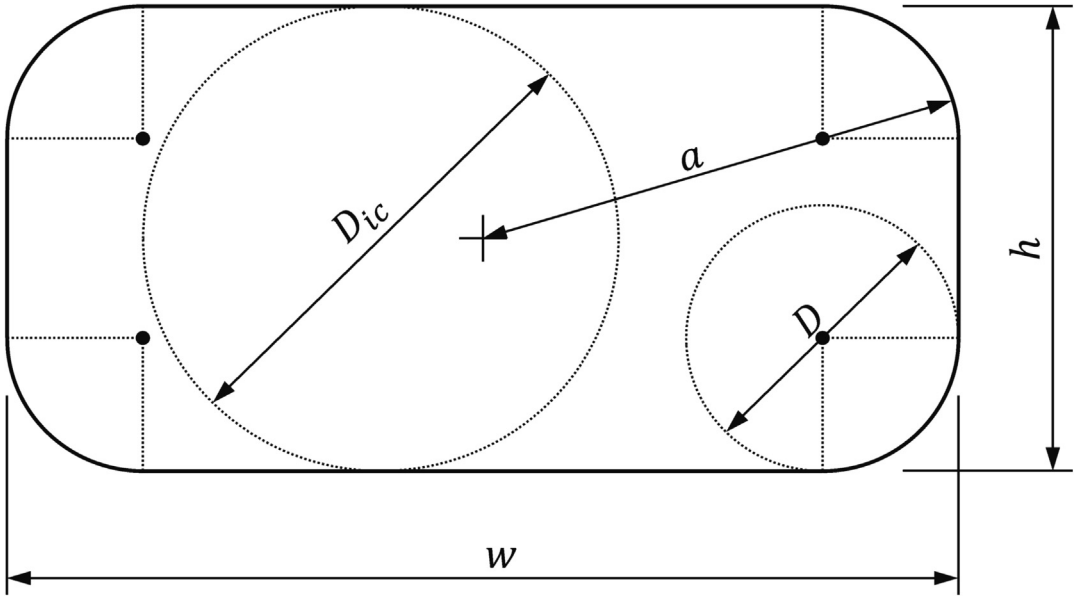


Fig. 5. Idealised particle outline to investigate the relationship between ellipseness E and overall particle form.

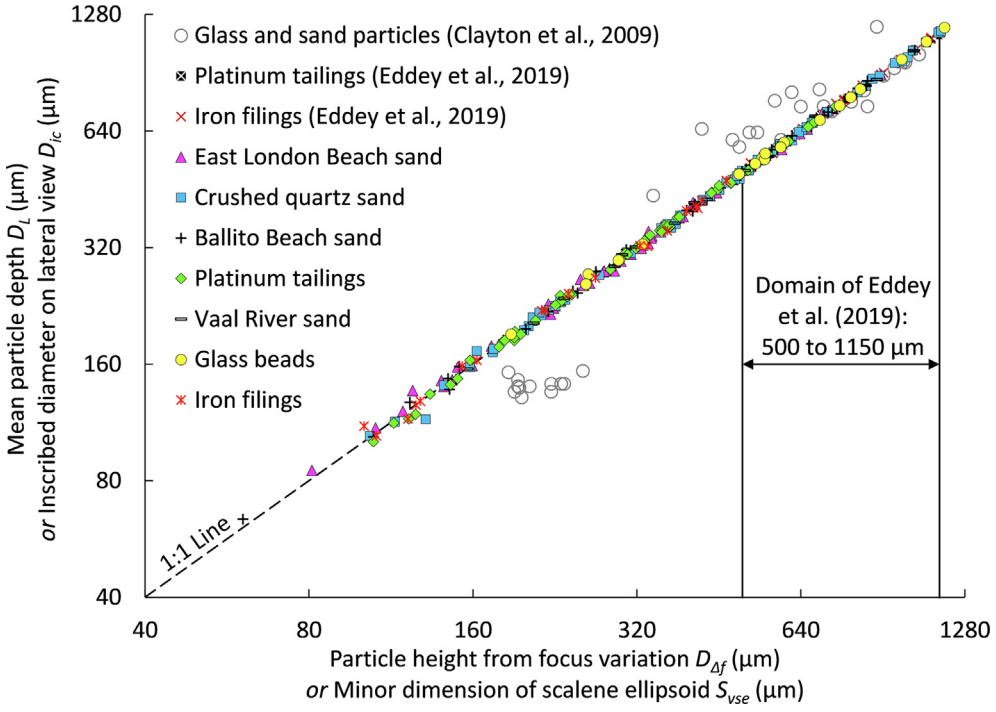


Fig. 6. Relationship between D_L and $D_{\Delta f}$ and between D_{ic} and S_{vse}.

edging that measurements of particle height from lateral views also have limited precision. Fig. 7 illustrates this by plotting the difference between the two particle height measurements based on lateral views ($D_{L2} - D_{L1}$) against the mean particle height D_L. Although D_{L1} and D_{L2} should be identical, experimental errors result in discrepancies with a mean value of ~3 µm which occasionally approach 25 µm. In the absence of additional measurements, it is reasonable to interpret D_{L1} and D_{L2} as a best estimate of the limits of the range within which the real, but unknown, particle height falls. Accordingly, the error (ε) of $D_{\Delta f}$ was computed according to Eq. (8). Essentially, ε was taken as zero when $D_{\Delta f}$ fell between D_{L1} and D_{L2}, positive when focus variation overestimated particle height ($D_{\Delta f} > D_{L2}$), and negative when focus variation underestimated particle height ($D_{\Delta f} < D_{L1}$).

$$\varepsilon = \begin{cases} D_{\Delta f} - D_{L2} & D_{L2} < D_{\Delta f} \\ 0 & D_{L1} \leq D_{\Delta f} \leq D_{L2} \\ D_{\Delta f} - D_{L1} & D_{\Delta f} < D_{L1} \end{cases} \quad (8)$$

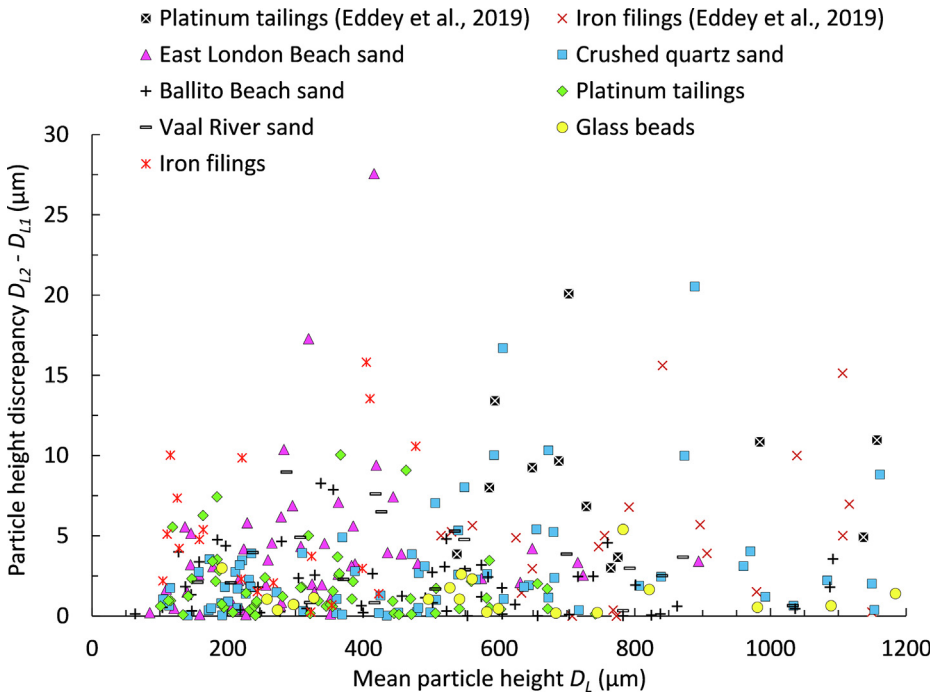


Fig. 7. Discrepancies between particle heights measured on two different lateral views.

Fig. 8a shows the error ε against the mean particle height D_L for the entire dataset. The ε values exhibit a symmetric distribution of data points around the $\varepsilon = 0$ line with a resulting mean and standard deviation of $\mu_\varepsilon = 0.04$-µm and $\sigma_\varepsilon = 4.6$ µm, respectively. The mean overestimation (3.9 µm) is virtually identical to the mean underestimation (-3.8 µm). These metrics show that the focus variation procedure is an unbiased estimator of particle height. Fig. 8a also shows that there is no systematic correlation between ε and D_L, and that the measurement errors of the iron filings are similar to the errors of the remainder of the dataset. The latter observation suggests that the thin layer of glue used to secure the non-magnetic particles to the prismatic base did not compromise the precision of the focus variation procedure. It is likely that the errors are at least partly due to the uncertainties introduced by operator subjectivity when performing the focus variations.

Because the DoF depends on the characteristics of the objective (Eq. (4), Table 2), it is of interest to explore whether the objective used has an effect on ε. Fig. 8b suggests that there is a slightly increased potential error ε at smaller magnifications. This is consistent with the fact that greater magnification typically corresponds to greater numerical aperture and thus a reduced DoF (Eq. (4), Table 2). It follows that for optimal results, the focus variation procedure should be implemented with the highest magnification possible.

Fig. 9 presents the absolute value of ε normalised by the mean particle height D_L. For reference, Fig. 9 also includes curves that consider an error ε of one and three times the standard deviation σ_ε. As expected, the potential for large relative errors increases as particle height decreases. However, 98 % of the entire dataset exhibits normalised absolute errors $\leq$ 5 %. As noted earlier, this precision is encouraging as it surpasses that of a previously proposed method (see comparison to Clayton et al. (2009) in Fig. 6). However, whether the precision of the focus variation procedure is acceptable for geotechnical purposes depends on whether its use leads to measurements of form that can be successfully correlated to the engineering behaviour of soils. For it is such behaviour which is the ultimate concern of geotechnical engineers. Notwithstanding, the establishment of correlations between form and engineering properties falls beyond the scope of the current work.

3.2. Assessments of form

Fig. 10 presents the results of particle form assessments on diagrams of I/L vs S/I as proposed by Zingg (1935) with superimposed contours of S/L. The results are presented on three different plots to minimise clutter. The cuboids on the corners of the Zingg diagrams provide a qualitative guide to interpret the results. Across all soiltypes, particles with $S/L < 0.2$ are relatively rare. These are particles that would exhibit plate-like, bladed or rod-like geometries. Furthermore, the glass beads (Fig. 10c) are the soiltype that plots the closest to the equant corner ($S/I = I/L = 1$), which is consistent with the approximately spherical geometry of the beads. Except for these commercially manufactured glass beads, all material types show significant scatter, which implies substantial variations in their form ratios S/I, I/L, and S/L. This highlights the importance of assessing form on multiple individual particles as opposed to adopting a single average form descriptor for a given mate-

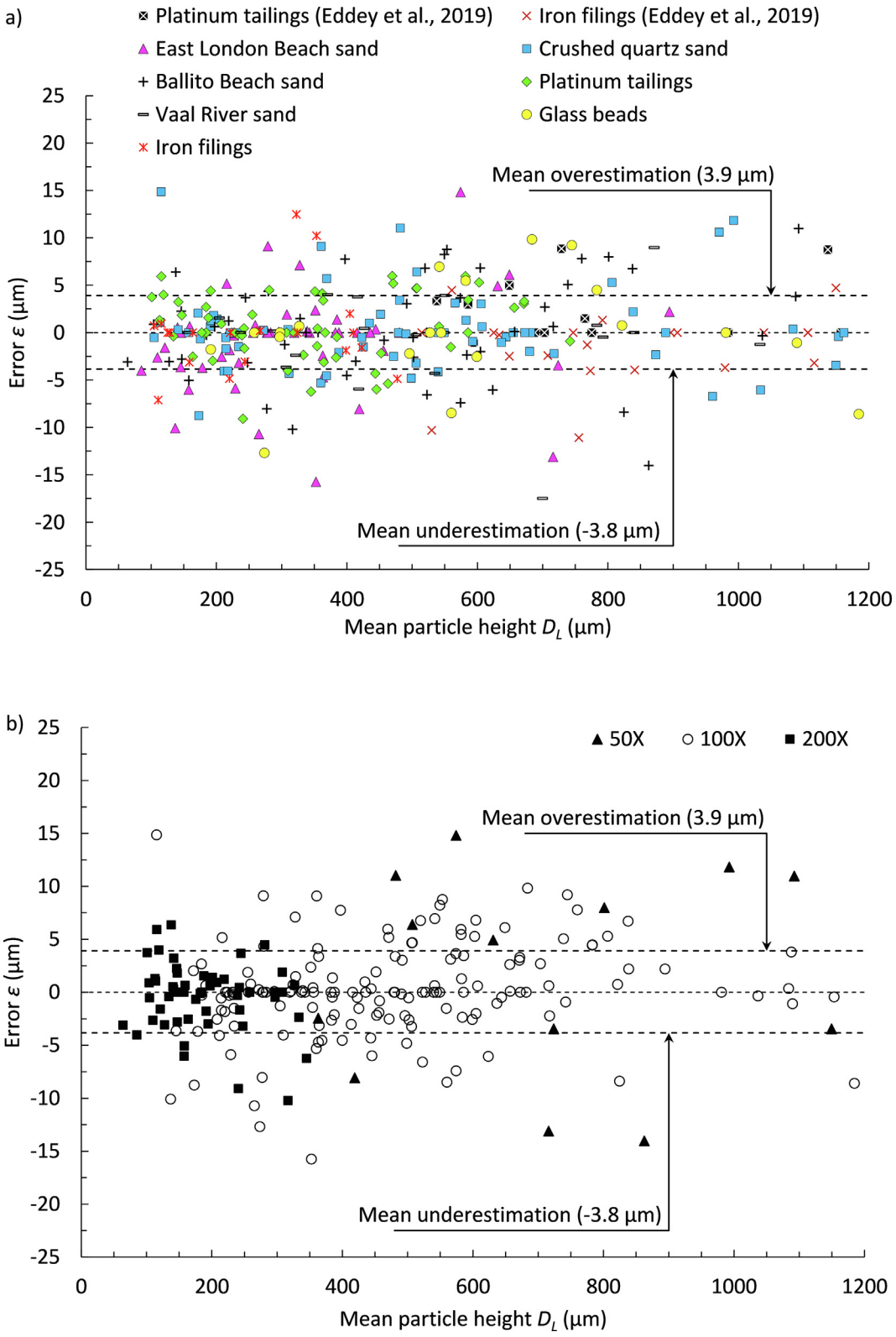


Fig. 8. Error ε in particle height with data discriminated by (a) material type and (b) magnification. Note: Part (b) does not include data from Eddey et al. (2019).

rial type as has been suggested previously (Kwan et al., 1999).

It is often of interest to determine whether there are any significant correlations between form and particle size (Le Pen et al., 2013; Wang et al., 2020). Exploring such a correlation requires adopting an unambiguous definition of particle size. The issue is not straightforward because, as highlighted by the form analyses, the irregular geometries

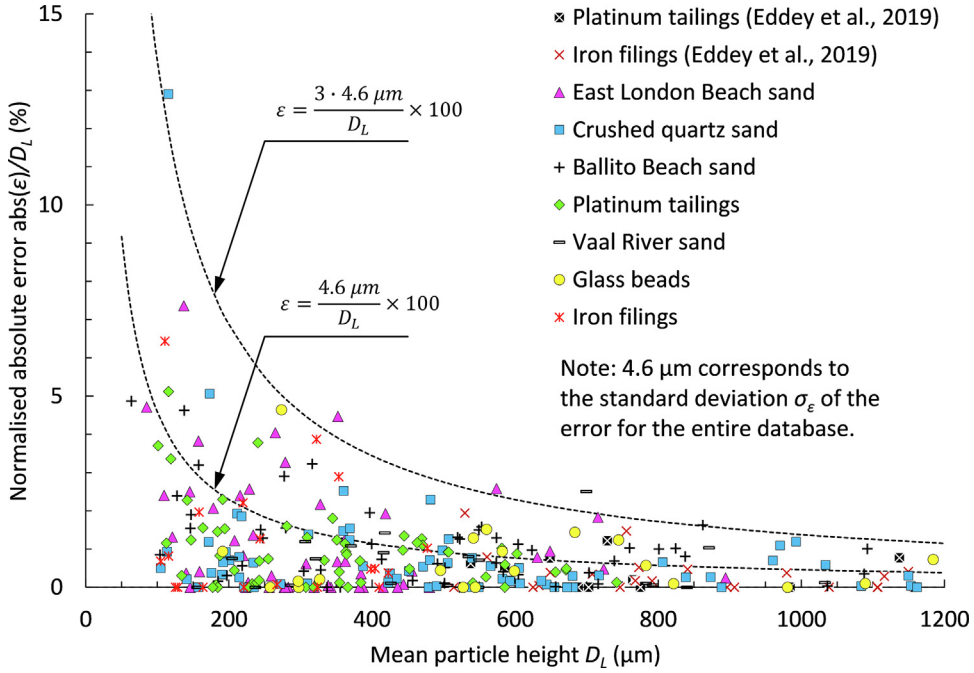


Fig. 9. Absolute error ε normalised by the mean particle height D_L.

of particles cannot be described by a single dimension. Previous studies have characterised particle size using the apertures of the sieves between which a particle is retained (Le Pen et al., 2013; Wang et al., 2020). However, this amounts to discretising a variable that is in effect continuous. We suggest that having measured S, I, and L, this discretisation can be avoided by adopting a Pythagorean definition of particle size (P) as shown in Eq. (9).

$$P = \sqrt{S^2 + I^2 + L^2} \tag{9}$$

None of the material types investigated herein exhibited significant correlations between the form ratios S/I, I/L, and S/L; and P. To illustrate the lack of correlation Fig. 11 presents the S/L vs P data of the sub-rounded East London Beach sand and the angular crushed quartz sand. This is in general agreement with previous researchers reporting only weak correlations between particle shape parameters and alternative definitions of particle size (Le Pen et al., 2013; Wang et al., 2020). Fig. 11 also shows that for a given soil and at any given particle size P, the form ratio S/L can vary significantly. For example, the crushed quartz sand exhibits approximately $0.25 \leq S/L \leq 0.7$ over most of the P domain considered. In fact, none of the six material types whose forms were assessed herein yielded results that supported the notion that form ratios (S/I, I/L or S/L) are approximately uniform for a given particle size. This observation is at odds with the scalene ellipsoid method (Clayton et al., 2009) which assumes that, for a given soiltype and within a limited particle size range, particle form is approximately constant.

3.3. Assessments of roundness R and ellipseness E

Fig. 12 shows the ellipseness values computed for the idealised particle contour presented in Fig. 5. Each data point represents one of the 121 ellipseness computations performed for a given roundness. The results are symmetric around the $h/w = 1$ line because a rectangle with a height-to-width ratio of, for instance, m:n yields the same E as a rectangle with the inverse ratio n:m. More intuitively, rotating the shape by 90° does not affect the calculation of E.

It is clear from Fig. 12 that overall form, as characterised by the height-to-width ratio h/w, affects ellipseness assessments since, for a given roundness R, there is a systematic and unique correlation between E and h/w. It is also evident that although both R and E are indicators of angularity, they are not uniquely correlated. Furthermore, although particles with $h/w < 0.1$ and $h/w > 10$ are not common in soils, this domain of the graph is instructive as it shows that the curves corresponding to different R values converge to similar E values. The implication is that for extreme values of h/w, the parameter E is similar for particles that have very different values of R.

Fig. 13 shows comparisons between R and E for real particles of five different soiltypes. Roundness values span virtually the entire theoretical range $0 \leq R \leq 1$. Conversely, all particles fall within the range $0.84 \leq E \leq 1$. The particles fall along a swath of the graph, rather than along a line, which is consistent with the non-unique correlation between R and E identified in Fig. 12.

The crushed quartz sand and the platinum tailings are largely indistinguishable from each other in terms of both

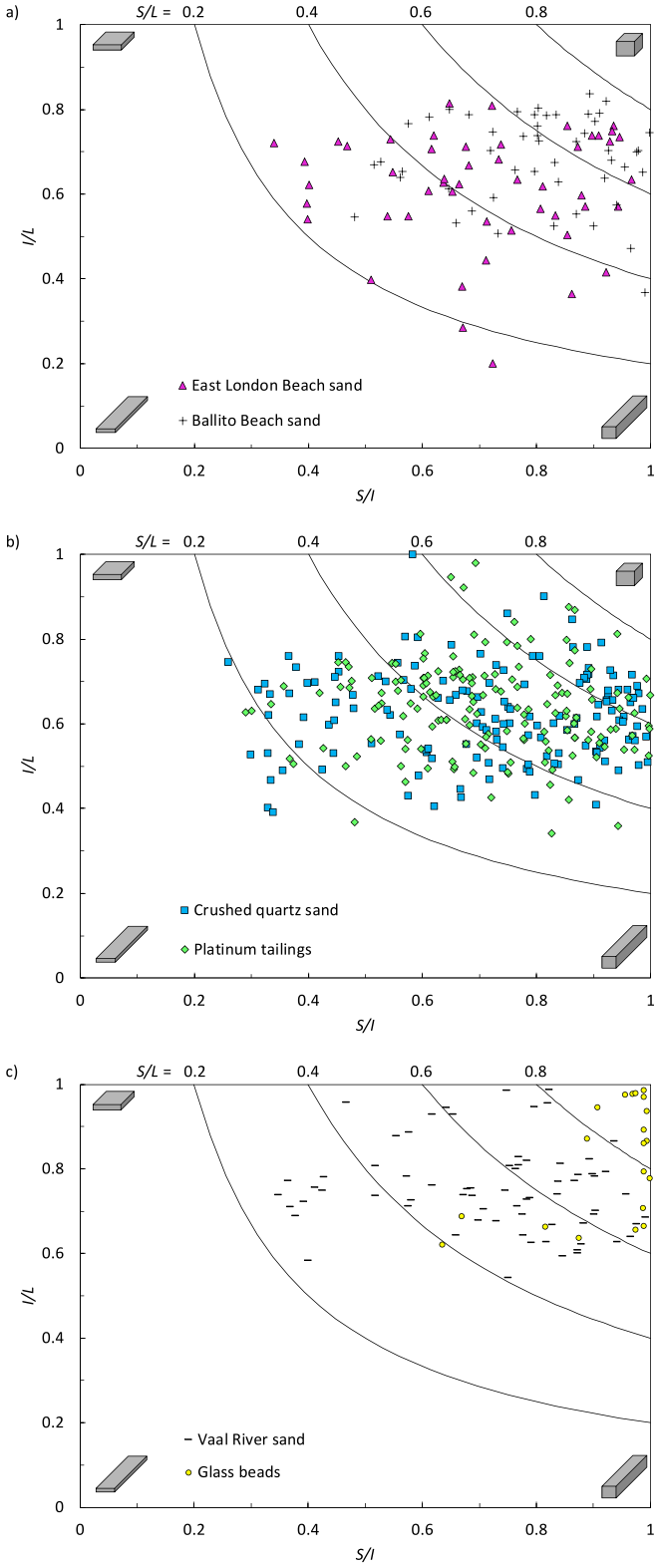


Fig. 10. Zingg diagrams for (a) East London Beach sand and Ballito Beach sand, (b) crushed quartz sand and platinum tailings, (c) Vaal River sand and glass beads.

roundness ($R \leq 0.2$) and ellipseness ($0.84 \leq E \leq 0.94$). This is consistent with the fact that both soils originate from a rock-crushing process that confers the particles a high angularity (Fig. 2c and 2d). Considering that these are angular particles, the range $0.84 \leq E \leq 0.94$ may seem surprisingly high. However, this range is similar to that of angular ballast obtained from rock crushing for which $0.84 \leq E \leq 0.98$ was reported (Le Pen et al., 2013).

The East London Beach sand and the Ballito Beach sand are also largely indistinguishable from each other in terms of both of roundness ($0.2 \leq R \leq 0.8$) and ellipseness ($0.94 \leq E \leq 1$). This is expected given commonalities in the formation processes of beach sands. As for the glass beads, they predominantly exhibit $R \geq 0.8$, which distinguishes them from the beach sands ($0.2 \leq R \leq 0.8$). However, in terms of ellipseness, the glass beads remain indistinguishable from the beach sands ($0.94 \leq E \leq 1$). These results suggest that while both R and E are suitable for distinguishing between predominantly angular and predominantly rounded particles, only R can distinguish between sub-rounded and well-rounded particles.

4. Conclusions

This work extended the validation of a focus variation procedure that exploits the limited depth of field of compound microscopes to measure the height of a particle without having to inspect a lateral view. The resulting measurements of particle height enabled the quantitative assessment of the form of six sand-sized material types. The procedure relies on simple tools (essentially a compound microscope and a dial indicator) to which many geotechnical researchers and practitioners are likely to have access. The procedure was validated by using adhesives or magnetic attraction to fix particles to a prismatic base. Additionally, the suitability of the 'ellipseness' parameter which had been previously proposed to assess angularity was also explored. Our results support the following conclusions:

a. For particle heights varying between 60 and 1200 μm, there is excellent agreement between the particle height as estimated from the focus variation procedure and particle height directly measured on lateral views. The particle height measurements are unbiased and exhibit an error distribution that has a standard deviation of 4.6 μm. There is no systematic correlation between the error and the particle height. Relative errors were smaller than 5 % for 98 % of all measurements. To minimise errors, the focus variation procedure should be implemented with the largest possible magnification as this yields a narrower depth of field that favours precision.
b. Successful measurements of particle height in sand-like materials from six different sources prove that the focus variation method is sufficiently robust to be applied across a wide variety of sand types.

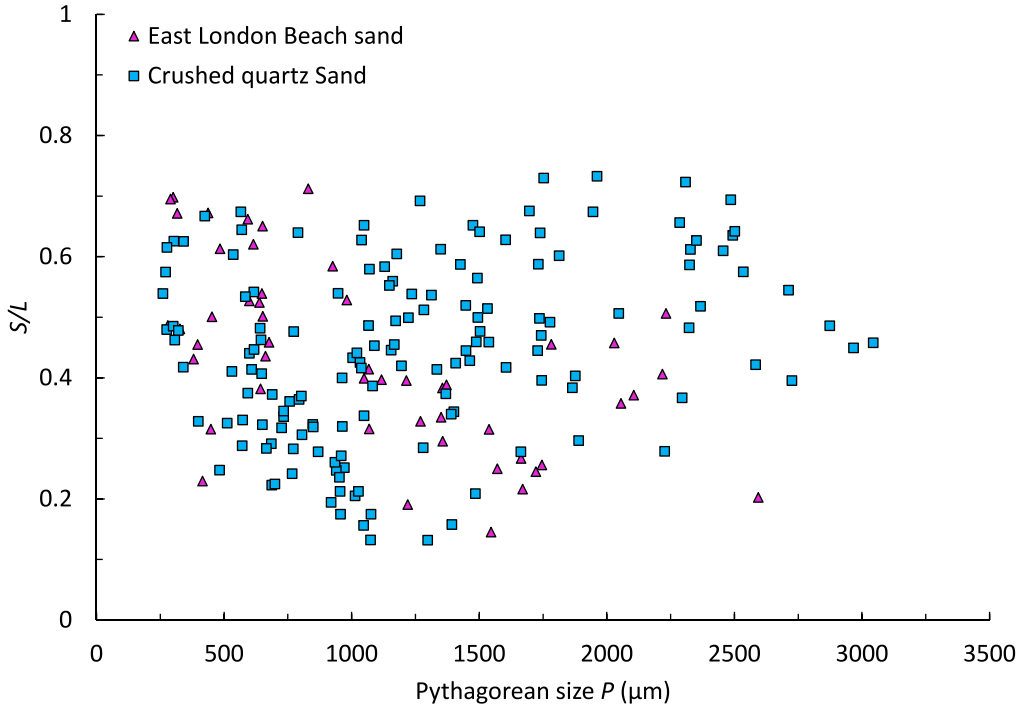


Fig. 11. Form ratio S/L against Pythagorean particle size P for East London Beach sand and crushed quartz sand.

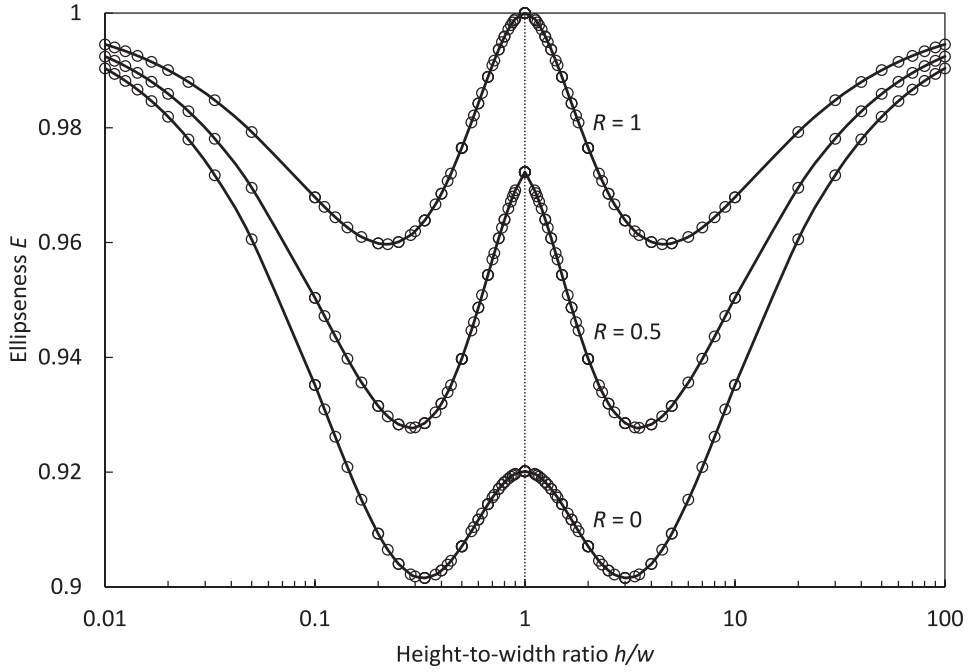


Fig. 12. Influence of the height-to-width ratio on ellipseness calculations for the idealised particle outline in Fig. 5.

c. There is significant variability of the form ratios S/I, I/L, and S/L amongst particles from the same type of sand. This variability remains even when considering particles of similar size. This result contradicts assumptions that have been adopted in previous studies. The sands considered herein did not exhibit a correlation between particle form and particle size.

d. The overall form of a particle outline influences its ellipseness E. Particles with very different values of Wadell's roundness R can yield very similar values of E if the height-to-width ratio of the particle outline exceeds 10. Although R and E are both indicators of angularity, these two parameters are not uniquely correlated.

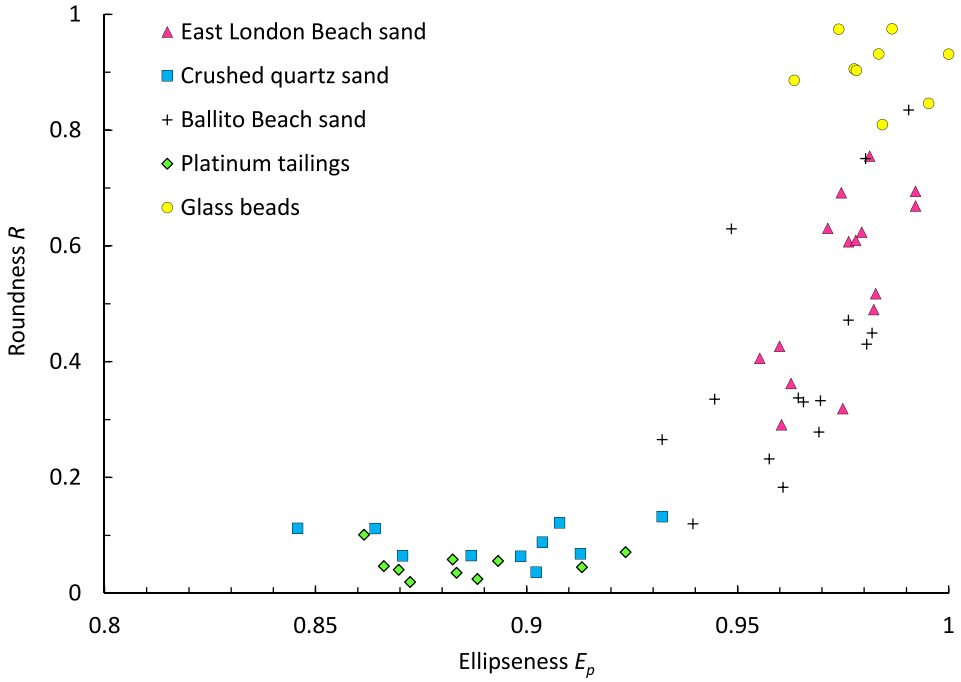


Fig. 13. Comparison of ellipseness and roundness for multiple particle types.

e. While, in principle, E can vary between 0 and 1, experimental results yielded $0.84 \leq E \leq 1$. These measurements included highly angular particles in which these values may appear unusually high. Both Wadell's roundness R and ellipseness E were able to distinguish between predominantly rounded and predominantly angular particles. However, only R was able to distinguish between sub-rounded and well-rounded particles.

Acknowledgements

Author contributions: M.B. conducted the initial feasibility investigation into particle form characterisation. C. E., L.T. and A.B. collected additional data, refined the validation procedure and incorporated angularity assessments. A.B. and L.A.T.C. prepared the first draft of the paper. L.A.T.C. contributed the original idea and supervised the project. This paper builds upon Bezuidenhout (2023). The authors thank Mr. D. Reddy and Professor Ziegler, from the Microscopy and Microanalysis Unit at the University of the Witwatersrand for useful discussions and their support in acquiring micrographs.

References

Alshibli, K.A., Druckrey, A.M., Al-Raoush, R.I., Weiskittel, T., Lavrik, N.V., 2014. Quantifying morphology of sands using 3-D imaging. J. Mater. Civ. Eng. 27 (10).

Aschenbrenner, B.C., 1956. A new method for expressing particle sphericity. J. Sed. Petrol. 26, 15–31.

ASTM, 2017. ASTM 2488-17E01 Standard practice for description and identification of soils (visual-manual procedure). West Conshohocken, PA, United States: ASTM International.

Barret, P.J., 1980. The shape of rock particles: a critical review. Sedimentology 27 (3), 291–303.

Bezuidenhout, A.W., 2023. Shape characterization of coarse particulates aided by focus variation microscopy. Research report for the degree of Master of Science in Engineering. University of the Witwatersrand, South Africa.

Blott, S., Pye, K., 2008. Particle shape: a review and new methods of characterization and classification. Sedimentology 55, 31–63.

Cho, G., Dodds, J., Santamarina, J., 2006. Particle shape effects on packing density stiffness and strength: natural and crushed sands. J. Geotech. Environ. Eng. ASCE 132 (5), 591–602.

Clayton, C.R.L., Abbireddy, C.O.R., Schiebel, R., 2009. A method of estimating the form of coarse particulates. Géotechnique 59 (6), 493–501.

Corey, A.T., 1949. Influence of shape on fall velocity of sand. MSc thesis, Colorado, A & M College.

Cruz-Matías, I., Ayala, D., Hiller, D., Gutsch, S., 2019. Sphericity and roundness computation for particles using the extreme vertices model. J. Comput. Sci. 30, 28–40.

Danzl, R., Helmli, F., Scherer, S., 2009. Focus variation - A new technology for high resolution optical 3D surface metrology. In: 10th International Conference of the Slovenian Society for Non-Destructive Testing: Application of Contemporary Non-Destructive Testing in Engineering. Ljubljana, Slovenia.

Dobkins Jr, J.E., Folk, R.L., 1970. Shape development on Tahiti-Nui. J. Sed. Petrol. 40, 1167–1203.

Eddey, C., Tiroyabone, L., Torres-Cruz, L. A., 2019. Three dimensional characterisation of the form of sand-sized particles. In: Proceedings of the 17th African Regional Conference on Soil Mechanics and Geotechnical Engineering. Cape Town, South Africa.

Fonseca, J., O'Sullivan, C., Coop, M., Lee, P., 2012. Non-invasive characterization of particle morphology of natural sands. Soils Found. 52 (4), 712–722.
Goodwin, P.C., 2015. A primer on the fundamental principles of light microscopy: optimising magnification, resolution, and contrast. Mol. Reprod. Dev. 82, 502–507.
Holtz, R.D., Kovacs, W.D., 1981. An Introduction to Geotechnical Engineering. Prentice-Hall Inc, Englewood Cliffs, New Jersey.
Inoué, S., Spring, K.R., 1997. Video Microscopy: The Fundamentals, second ed. Plenum Press, New York.
ISO., 2020. ISO 10934:2020 Microscopes – Vocabulary for light microscopes. International Organization for Standardization.
Janoo, V. C., 1998. Quantification of Shape, Angularity, and Surface Texture of Base Course Materials.
Jumelle, C., Hamri, A., Egaud, G., Mauclair, C., Reynaud, S., Dumas, V., Pereira, S., Garcin, T., Gain, P., Thuret, G., 2017. Comparison of four methods of surface roughness assessment of corneal stromal bed after lamellar cutting. Biomed. Opt. Express 8 (1), 4974–4986.
Krumbein, W., 1941. Measurement and geological significance of shape and roundness of sedimentary particles. J. Sed. Petrol. 11, 64–72.
Krumbein, W.C., Sloss, L.L., 1963. Stratigraphy and Sedimentation. Freeman and Company, San Francisco.
Kwan, A.K.H., Mora, C.F., Chan, H.C., 1999. Particle shape analysis of coarse aggregate using digital image processing. Cem. Concr. Res. 29, 1403–1410.
Le Pen, L.M., Powrie, W., Zervos, A., Ahmed, S., Aingaran, S., 2013. Dependence of shape on particle size for a crushed rock railway ballast. Granular Matter. 15, 849–861.
Lee, J.R.J., Smith, M.L., Smith, L.N., 2007. A new approach to the three-dimensional quantification of angularity using image analysis of the size and form of coarse aggregates. Eng. Geol. 91 (2), 254–264.
Liang, H., Shen, Y., Xu, J., Shen, X., 2021. Multiscale three-dimensional morphological characterisation of calcareous sand particles using spherical harmonic analysis. Front. Phys. 9 744319.
Masad, E. A., 2005. Aggregate Imaging System (AIMS): Basics and Applications. Report for the Texas Transportation Institute.
Mgangira, M., Anochie-Boateng, J. K., Komba, J., 2013. Quantification of Aggregate Grain Shape Characterisation using 3-D Laser Scanning Technology, 32nd South African Transportation Conference. Pretoria, South Africa.
Nie, Z., Liang, Z., Wang, X., 2018. A three-dimensional particle roundness evaluation method. Granular Matter. 20 (32).
Orford, J.D., Whalley, W.B., 1983. The use of the fractal dimension to quantify the morphology of irregular-shaped particles. Sedimentology. 30, 655–668.
Powers, M.C., 1953. A new roundness scale for sedimentary particles. J. Sed. Petrol. 23, 117–119.
Pye, W., Pye, M., 1943. Sphericity determination of pebbles and sand grains. J. Sed. Petrol. 13, 28–34.
Ramanujan, S., 1914. Modular equations and approximations to π. Q. J. Pure Ppl. Math. 45, 350–372.
Riley, N.A., 1941. Projection sphericity. J. Sed. Petrol. 11, 94–97.
Scherer, S., 2007. Focus-Variation for optical 3D measurement in the micro- and nano-range, Handbuch zur Industriellen Bildverarbeitung: Qualitätssicherung in der Praxis. Fraunhofer IRB Verlag,
Shin, H., Santamarina, J.C., 2013. Role of particle angularity on the mechanical behaviour of granular mixtures. J. Geotech. Geoenviron. 139, 353–355.
Sneed, E., Folk, R., 1958. Pebbles in the Lower Colorado River, Texas: a study in particle morphogenesis. J. Geol. 66 (2), 114–150.
Sun, Y., Indraratna, B., Nimbalkar, S., 2014. Three-dimensional characterisation of particle size and shape for ballast, Faculty of Engineering and Information Sciences - Papers: Part A, University of Wollongong.
Wadell, H., 1932. Volume, shape and roundness of rock particles. J. Geol. 40, 443–451.
Wadell, H., 1933. Sphericity and roundness of rock particles. J. Geol. 27, 507–521.
Wang, X., Wu, Y., Cui, J., Zhu, C., Wang, X., 2020. Shape characteristics of coral sand from the South China Sea. J. Marine Sci. Eng. 8 (10).
Wentworth, C.K., 1922. The shapes of beach pebbles. US Geol. Surv. Prof. Pap. 131-C, 75–83.
Yu, L., Gong, F., You, Z., Wang, H., 2018. Aggregate morphological characterisation with 3D optical scanner vs X-ray computed tomography. J. Mater. Civil Eng. 30 (1).
Zhao, B., Wang, J., Coop, M.R., Viggiani, G., Jiang, M., 2015. An investigation of single sand particle fracture using X-ray micro tomography. Géotechnique. 65 (8), 625–641.
Zhou, B., Wang, J.F., 2016. Generation of a realistic 3D sand assembly using X-ray micro-computed tomography and spherical harmonic-based principal component analysis. Int. J. Numer. Anal. Meth. Geomech. 41, 93–109.
Zhou, B., Wang, J., Wang, H., 2018. Three-dimensional sphericity, roundness and fractal dimension of sand particles. Géotechnique. 68 (1), 18–30.
Zingg, T., 1935. Beitrage Zur Schootteranalyse. Schweizminer. Petrog. Mitt. 15, 38–140.